PUNE RESEARCH DISCOVERY ISSN 2455-9202
AN INTERNATIONAL JOURNAL OF ADVANCED STUDIES VOL 2, ISSUE 2

UNSTEADY CONVECTIVE HEAT TRANSFER OF A VISCOUS FLUID THROUGH A POROUS MEDIUM IN A VERTICALCHANNEL WITH QUADRATIC TEMPERATURE VARIABLE

DR. K. GNANESWAR
Principal,
S.K.P. Government Degree College,
Guntakal, Anantapuramu-Dist, (AP) **INDIA**

ABSTRACT

We make an investigation of the radiation effect on an unsteady mixed convection heat transfer through a porous medium confined in a vertical channel on whose walls a traveling thermal wave in imposed-in the presence of the heat sources. The equations governing the flow and heat transfer which are non-linear and coupled have been solved by applying a regular perturbation technique with the aspect ratio δ as a perturbation parameter. The effect of radiation on the entire flow characteristic has been shown by graphical representations of the velocity, temperature, shear stress and Nusselt number.

Keywords: *Unsteady; Heat transfer; Viscous fluid; Vertical channel; Quadratic temperature variable; Perturbation technique.*

INTRODUCTION:

The energy crisis has been a topic of great importance in recent years all over the world. This has resulted in an unabated exploration for new ideas and avenues in harnessing various conventional energy sources like tidal waves, wind power and geothermal energy. It is well known that in order to harness maximal geothermal energy one should have complete and precise knowledge of quanta of perturbation needed to initiate convection currents in mineral fluids embedded in the earth's crest enables one to use mineral energy to extract the minerals. For example, in the recovery of hydrocarbons from underground petroleum reservoirs, the use of thermal processes is becoming important to enhance the recovery. Heat can be injected into the reservoir as hot water or stream or heat can be generated institute by burning part of the reservoir crude. In all such thermal recovery processes fluid flow takes place through a porous medium and convection flow through a porous medium at most important, determination of the external energy required to initiate convection currents needs a through

understanding of convective processes in a porous medium. There has been a great quest in Geophysicists to study the problem of convection currents in a porous medium heated from below.

Transport of Momentum and thermal energy in fluid saturated porous media with low porosities were commonly described by Darcy's model for conservation of momentum and by an energy equation based on the velocity field found from Kaviancy (6). In contrast to rocks, soil, sand and other media that do fall in this category, usually have high porosity. Vajravelu (9) examined the steady flow that of heat transfers in a porous medium with high porosity. Raptis (7) studied mathematically the case of time varying two-dimensional natural convective heat transfer of an incompressible electrically conducting viscous fluid through a high porous medium bounded by an infinite vertical porous plate. Jaiswal and Soundalgekhar (4) studied the natural convection in a porous medium with high porosity.

Convection fluid flows generated by traveling thermal waves have also received attention due to applications in physical problems. The linearised analysis of these flows has shown that a traveling thermal wave can generate a mean shear flow with in a layer of fluid and the induced mean flow is proportional to the square of the amplitude of the wave. From a physical point of view, the motion induced by traveling thermal wave is quite interesting as a purely fluid dynamical problem and can be used as a possible explanation for the observed Four-day retrograde zonal motion of the upper atmosphere of Venus. Also, the heat transfer results will have a definite bearing on the design of oil or gas fired boilers.

Vajravelu and Debnath (9) have made an interesting study of non-linear convection heat transfer and fluid flows, induced by traveling thermal wave. The traveling thermal wave's problem was investigated both analytically and experimentally by Whitehead (10) by posulating series expansion in the square of the aspect ratio (assumed small) for both the temperature and flow fields. Whitehead (10) obtained an analytical solution for the mean flow produced by a moving source theoretically predictions regarding the ratio of the mean flow velocity to the source speed were found to be in good agreement with experimental observations in mercury which therefore justified validity of the asymptotic expansion a posteriori. Ravindra (8) has analyzed the mixed convection flow of a viscous fluid through a porous medium in a vertical channel. The thermal buoyancy medium in the flow field is created by a traveling thermal wave imposed on the boundaries.

Recently Bharathi (1) has investigated the radiation effect on convective heat transfer through a porous in a vertical channel with traveling thermal wave. In all the above a linear density variations is considered in the equation of state. This is valid for temperature variation at 20^0C. But this analysis is not applicable to the study of the flow of water at 4^0C. The density of water is maximum at atmospheric pressure and the modified form of the equation to water at 4^0c is given by

$$\Delta\rho = - \rho\gamma (\Delta T)^2$$

where $\gamma = 8 \times 10^{-6} (0c)^{-2}$. Taking this fact into account, Goren (2) showed in this case similarity solution for the free convection flow of water at 4^0c past a semi-finite vertical plate exists. Govindarajulu (3) showed that a similarity solution exists for the free convection flow of water at 4^0C from vertical and horizontal plates in the presence of suction and injection. Recently Jaffarunissa (5) has studied unsteady MHD convection heat transfer of a viscous electrically conducting fluid in a vertical channel with traveling thermal wave imposed on the walls.

In this chapter we make an investigation of the radiation effect on an unsteady mixed convection heat transfer through a porous medium confined in a vertical channel on whose walls a traveling thermal wave in imposed-in the presence of the heat sources. The equations governing the flow and heat transfer which are non-linear and coupled have been solved by applying a regular perturbation technique with the aspect ratio δ as a perturbation parameter. The effect of radiation on the entire flow characteristic has been shown by graphical representations of the velocity, temperature, shear stress and Nusselt number.

2. FORMULATION OF THE PROBLEM

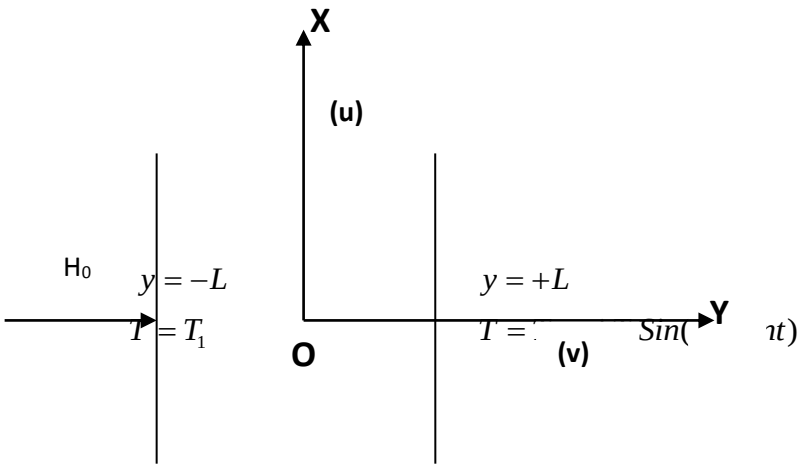

Fig.3 Schematic diagram of the flow configuration

We consider the motion of viscous, fluid through a porous medium in a vertical channel bounded by flat walls. The thermal buoyancy in the flow field is created by a traveling thermal wave imposed on the boundary wall at y=L while the boundary at y= -L is maintained at constant temperature T_1. The Boussinesq approximation is used so that the density variation will be considered only in the buoyancy force. Also the kinematic viscosity ν, the thermal conducting k are treated as constants. We choose a rectangular Cartesian system 0(x, y) with x-axis in the vertical direction and y-axis normal to the walls. The walls of the channel are at y= ±L. The equations governing the unsteady flow and heat transfer are

Equation of linear momentum

$$\rho_e\left(\frac{\partial u}{\partial t}+u\frac{\partial u}{\partial x}+v\frac{\partial u}{\partial y}\right)=-\frac{\partial p}{\partial x}+\mu\left(\frac{\partial^2 u}{\partial x^2}+\frac{\partial^2 u}{\partial y^2}\right)-\rho g-\left(\frac{\mu}{k}\right)u-\left(\frac{\sigma\mu_e^2 H_o^2}{\rho_e}\right)u \tag{4.1}$$

$$\rho_e\left(\frac{\partial v}{\partial t}+u\frac{\partial v}{\partial x}+v\frac{\partial v}{\partial y}\right)=-\frac{\partial p}{\partial y}+\mu\left(\frac{\partial^2 v}{\partial x^2}+\frac{\partial^2 v}{\partial y^2}\right)-\left(\frac{\mu}{k}\right)v \tag{4.2}$$

Equation of continuity

$$\frac{\partial u}{\partial x}+\frac{\partial v}{\partial y}=0 \tag{4.3}$$

Equation of energy

$$\rho_e C_p\left(\frac{\partial T}{\partial t}+u\frac{\partial T}{\partial x}+v\frac{\partial T}{\partial y}\right)=\lambda\left(\frac{\partial^2 T}{\partial x^2}+\frac{\partial^2 T}{\partial y^2}\right)+Q-\frac{\partial q_r}{\partial y} \tag{4.4}$$

Equation of state

$$\rho-\rho_e=-\beta\rho_e(T-T_e)^2 \tag{4.5}$$

where ρ_e is the density of the fluid in the equilibrium state, T_e is the temperature and in the equilibrium state, (u, v) are the velocity components along O(x, y) directions, p is the pressure, T is the temperature in the flow region, ρ is the density of the fluid, μ is the constant coefficient of viscosity, Cp is the specific heat at constant pressure, λ is the coefficient of thermal conductivity, k is the permeability of the porous medium, β is the coefficient of thermal expansion, r is the radiative heat flux and Q is the strength of the constant internal heat source.

Invoking Rosseland approximation (Brewester (1a)) for the radiative flux we get

$$q_r=\frac{4\sigma^{\bullet}}{3\beta_R}\frac{\partial(T'^4)}{\partial y} \tag{4.6}$$

expanding T'^4 in Taylor series about T_e and neglecting higher order terms (19a),

$$T'^4\approx 4TT_e^3-3T_e^4 \tag{4.7}$$

where $\sigma^{\bullet}$ is the Stefan-Boltzman constant and β_R is the mean absorbing coefficient.
In the equilibrium state

$$0=-\frac{\partial p_e}{\partial x}-\rho_e g \tag{4.8}$$

where $p=p_e+p_D$, p_D being the hydrodynamic pressure.
The flow is maintained by a constant volume flux for which a characteristic velocity is defined as

$$Q = \frac{1}{2L}\int_{-L}^{L} u\, d\, y \quad . \tag{4.9}$$

The boundary conditions for the velocity and temperature fields are

$$u = 0,\ v = 0,\ T = T_1 \qquad \text{on } y = -L$$
$$u = 0,\ v = 0,\ T = T_2 + \Delta T_e\, Sin(mx + nt) \qquad \text{on } y = L \tag{4.10}$$

where $\Delta T_e = T_2 - T_1$ and $Sin(mx + nt)$ is the imposed traveling thermal wave

In view of the continuity equation we define the stream function ψ as

$$u = -\psi_y,\ v = \psi_x \tag{4.11}$$

Eliminating pressure p from equations (4.2) & (4.3) and using the equations governing the flow in terms of ψ are

$$[(\nabla^2\psi)_t + \psi_x(\nabla^2\psi)_y - \psi_y(\nabla^2\psi)_x] = \nu\nabla^4\psi - 2\beta\, g(T - T_0)(T - T_0)_y - (\frac{\nu}{k})\nabla^2\psi - (\frac{\sigma\mu_e^2 H_o^2}{\rho_e})\frac{\partial^2\psi}{\partial y^2} \tag{4.12}$$

$$\rho_e C_p\left(\frac{\partial\theta}{\partial t} + \frac{\partial\psi}{\partial y}\frac{\partial\theta}{\partial x} - \frac{\partial\psi}{\partial x}\frac{\partial\theta}{\partial y}\right) = \lambda\nabla^2\theta + Q + \frac{16\sigma^{\bullet}T_e^3}{3\beta_R}\frac{\partial^2 T}{\partial y^2} \tag{4.13}$$

Introducing the non-dimensional variables in (4 .12) & (4.13) as

$$x' = mx,\ y' = y/L,\ t' = t\nu m^2,\ \Psi' = \Psi/\nu,\ \theta = \frac{T - T_2}{T_1 - T_2} \tag{4.14}$$

the governing equations in the non-dimensional form (after dropping the dashes) are

$$\delta R(\delta(\nabla_1^2\psi)_t + \frac{\partial(\psi, \nabla_1^2\psi)}{\partial(x, y)}) = \nabla_1^4\psi + \frac{2G}{R}(\theta\,\theta_y) - D^{-1}\nabla_1^2\psi - M^2\frac{\partial^2\psi}{\partial y^2} \tag{4.15}$$

The energy equation in the non-dimensional form is

$$\delta P_1\left(\delta\frac{\partial\psi}{\partial t} - \frac{\partial\psi}{\partial y}\frac{\partial\theta}{\partial x} + \frac{\partial\psi}{\partial x}\frac{\partial\theta}{\partial y}\right) = \nabla_1^2\theta + \alpha_1 \tag{4.16}$$

where

$R = \frac{UL}{\nu}$ (Reynolds number)

$G = \frac{\beta\, g\Delta T_e L^3}{\nu^2}$ (Grashof number)

$M^2 = \frac{\sigma\mu_e^2 H_o^2 L^2}{\nu^2}$ (*Hartmann Number*)

$P = \frac{\mu C_p}{k_1}$ (Prandtl number),

$D^{-1} = \frac{L^2}{k}$ (Darcy parameter),

$\delta = m L$ (Aspect ratio)

$\gamma = \frac{n}{\nu m^2}$ (Non-dimensional thermal wave velocity)

$N = \frac{\beta_R \lambda}{4\sigma^{\bullet} T_e^3}$ (Radiation parameter)

$P_1 = \frac{3NP}{3N+4}$ $\alpha_1 = \frac{3N\alpha}{3N+4}$

$\nabla_1^2 = \delta^2 \frac{\partial^2}{\partial x^2} + \frac{\partial^2}{\partial y^2}$

The corresponding boundary conditions are

$$\psi(+1) - \psi(-1) = 1$$

$$\frac{\partial \psi}{\partial x} = 0, \quad \frac{\partial \psi}{\partial y} = 0 \quad at\ y = \pm 1 \qquad (4.17)$$

$\theta(x, y) = 1$ on y = -1

$\theta(x, y) = Sin(x + \gamma t)$ on y = 1

$$\frac{\partial \theta}{\partial y} = 0 \quad at \quad y = 0 \qquad (4.18)$$

The value of ψ on the boundary assumes the constant volumetric flow in consistent with the hypothesis (4.9) .Also the wall temperature varies in the axial direction in accordance with the prescribed arbitrary function t

3. ANALYSIS OF THE FLOW

The main aim of the analysis is to discuss the perturbations created over a combined free and forced convection flow due to traveling thermal wave imposed on the boundaries. The perturbation analysis is carried out by assuming that the aspect ratio δ to be small.

We adopt the perturbation scheme and write

$$\psi(x, y) = \psi_0(x, y) + \delta\psi_1(x, y) + \delta^2\psi_2(x, y) +$$
$$\theta(x, y) = \theta_0(x, y) + \delta\theta_1(x, y) + \delta^2\theta_2(x, y) + \qquad (4.19)$$

On substituting (4.19) in (4.15) & (4.16) and separating the like powers of δ the equations and respective conditions to the zeroth order are

$$\psi_{0,\,yyyyy} - M_1^2 \psi_{0,\,yy} = -2G(\theta_o\, \theta_{0,y})/R \qquad (4.20)$$

$$\theta_{o,yy} = -\alpha_1 \qquad (4.21)$$

with

$$\psi_0(+1)\text{-}\Psi(-1) = 1,$$
$$\psi_{0,y} = 0,\ \psi_{0,x} = 0 \qquad \text{on } y = \pm 1 \qquad (4.22)$$
$$\theta_o = 1 \qquad on \quad y = -1$$

$$\theta_o = Sin(x + \gamma t) \qquad on\ y = 1 \qquad (4.23)$$

and to the first order are

$$\psi_{1,\,yyyyy} - M_1^2 \psi_{1,\,yy} = -2G(\theta_o \theta_{1,yy} + \theta_1\, \theta_{o,y})/R + (\psi_{0,\,y}\, \psi_{0,\,xyy} - \psi_{0,\,x}\, \psi_{0,yyy}) \qquad (4.24)$$

$$\theta_{1,yy} = P_1(\psi_{0,x}\theta_{o,y} - \psi_{0,y}\theta_{ox}) \qquad (4.25)$$

$$\psi_{1,y} = 0\,, \quad \psi_{1,x} = 0 \qquad \text{on } y = \pm 1 \qquad (4.26)$$

$$\theta_1(\pm 1) = 0\,, \qquad \text{on } y = \pm 1 \qquad (4.27)$$

Solving the equations (4.20) & (4.21). (4.24) & (4.25) subject to the relevant boundary conditions (4.22), (4.23)(4.26) & (4.27) we obtain

$$\theta_o(y,t) = (\frac{\alpha}{2})(1-y^2) + (\frac{Sin(D_1)-1}{2})y + (\frac{Sin(D_1)+1}{2})$$

$$\psi_o(y,t) = a_{10} + a_{11}y + a_{12}Ch(M_1y) + a_{13}Sh(M_1y) + a_5y^3 + \phi(y)$$

$$\phi(y) = a_6y^2 + a_7y^3 + a_8y^4 + a_9y^5$$

$$\theta_1(y,t) = a_{16}(y^2-1)/2 + a_{17}(y^3-y)/6 + a_{18}(y^4-1)/12 + a_{19}(y^5-y)/20 +$$

$$+ a_{20}(y^6-1)/30 + a_{21}(y^7-y)/42 + a_{22}(y^8-1)/56$$

$$\psi_1 = B_1 + B_2y + B_3Ch(M_1y) + B_4Sh(M_1y) + \phi_1(y)$$

$$\phi_1(y) = -a_{55}y^2 a_{56}y^3 - a_{57}y^4 - a_{58}y^5 - a_{59}y^6 - a_{60}y^7 - a_{61}y^8$$

$$- a_{62}y^{10} + (ya_{63} + y^2a_{65} + y^3a_{67} + y^4a_{69} + y^5a_{71} + y^6a_{73})Ch(M_1y)$$

$$+ (ya_{64} + y^2a_{66} + y^3a_{68} + y^4a_{70} + y^5a_{72} + y^6a_{74})Sh(M_1y)$$

where $a_1, a_2, \ldots\ldots\ldots a_{74}, B_1, B_2, \ldots\ldots\ldots B_4$ *are constants given in the appendix*

The shear stress on the channel walls is given by

$$\tau = \mu\left(\frac{\partial u}{\partial y} + \frac{\partial v}{\partial x}\right)_{y = \pm L}$$

which in the non- dimensional form reduces to

$$\tau = (\frac{\tau}{\frac{\mu U}{a}}) = (\psi_{yy} - \delta^2 \psi_{xx})$$
$$= [\psi_{0,yy} + +\delta\psi_{1,yy} + O(\delta^2)]_{y=\pm 1}$$

and the corresponding expressions are

$$(\tau)_{y=+1} = a_{79} + \delta(a_{81} + a_{82}Ch(M_1))Cth(M_1) + a_{83}Ch(M_1) + a_{84}Sh(M_1) + a_{85}$$

$$(\tau)_{y=-1} = a_{80} + \delta(a_{86} + a_{87}Ch(M_1))Cth(M_1) + a_{88}Ch(M_1) + a_{89}Sh(M_1) + a_{90}$$

The local rate of heat transfer coefficient (Nusselt number Nu) on the walls has been calculated using the formula

$$Nu = \frac{1}{\theta_m - \theta_w}(\frac{\partial \theta}{\partial y})_{y=\pm 1}$$

and the corresponding expressions are

$$(Nu)_{y=+1} = \frac{(a_{93} + \delta a_{95})}{(a_{97} - Sin(D_1)}$$

$$(Nu)_{y=-1} = \frac{(a_{94} + \delta a_{96})}{(a_{97} - 1)}$$

where a_{75},…….a_{97} constants given in the appendix.

4. NUMERICAL RESULS

In this analysis we discuss the radiation effect on the convective heat transfer through a porous medium confined in a vertical channel on whose walls a traveling thermal wave is imposed with quadratic density temperature variation. The velocity and the temperature distributions are analyzed for different sets of parameter G, R, D^{-1}, α ,γ and $x + \gamma t$ and are represented in figures 1 - 12. In the following discussion we use the notations that the channel walls are heated or cooled according as G>0 or G<0. We take $\delta = 0.01$ and p=0.71 $\beta = 0.71$. It is to be noted that the temperature variation on the boundary contributes substantially to the flow field. This contribution may be represented as perturbation over the mixed convection flow generated in the state of uniform wall temperature; the perturbation not only depends on the wall temperature variation, but also on the nature of the mixed convection flow. It may be noted in general that creation of the reversal flow zone in the flow field depends on whether

the free convection effects dominates over the forced flow or vice –versa. If the free convection effects are sufficiently large as to create reversal flow the variation in the wall temperature affects the flow pattern remarkably.

Fig 1 represents the variation of the axial velocity (u) with Grashof number G. u<0 is the actual axial flow and u>0 is the reversal flow. It is found that no reversal flow exists anywhere in the flow region for any variation. The magnitude of u experiences an enhancement everywhere in the flow region with G>0 and depreciates with G<0. The maximum |u| occurs at y=-0.4 and at y=0.6 for G<0. From fig 2 we notice that lesser the permeability of the porous medium D^{-1} larger |u| in the left half and smaller |u| in the right half. An increase in thermal wave velocity γ enhances |u| in the left half and reduces |u| in the right half of the channel. The behavior of u with Reynolds number R reveals that |u| enhances in the region $-0.8 \le y \le 0.2$ and reduces in the regions $0 \le y \le 0.8$ with increase in R. From fig.3 we find that |u| enhances in the left half and reduces in the right half with $\alpha > 0$. An increase in the phase $x + \gamma t \le \pi$ leads to an enhancement in |u| and reduces with higher $x + \gamma t > \pi$ except in the vicinity of y =-1, (fig.4).

The secondary velocity (v) which arises due to the non-uniform temperature on the boundaries is shown in fig 5 – 8. It is found that for G>0 the secondary velocity is directed towards the boundary and is towards the mid region for G<0. |v| enhances with increase in G>0 and an increase in $|G| \le 2 \times 10^3$, |v| reduces in the left half and enhances in the right half and for higher $|G| \ge 3 \times 10^3$, |v| experiences an enhancement in the entire flow field. From fig. 6 shows that the variation of v with D^{-1} shows that lesser the permeability of the porous medium larger |v| in the left half of the flow region and in the right half |v| reduces with $D^{-1} \le 2 \times 10^2$ and enhances with higher $D^{-1} \ge 3 \times 10^2$ enhances near the boundaries and enhances with higher $R \ge 140$. An increase in the thermal wave velocity γ enhances |v| left half and reduces in the right half of the channel. The behavior of v with R shows that an increase in $R \le 70$ results in a depreciation in |v| in the central region (-0.2, 0.6). Fig-7 represents the variation of v with heat source parameter α. We find that the secondary velocity v is directed towards the boundary for α >0 and for α =-2 and for $|\alpha| \ge 4$, the velocity in the region $-0.8 \le y \le 0.2$ is towards the mid region and it is towards the boundary in the remaining region |v| experiences an enhancement with increase in the strength of the heat source/sink $|\alpha| \le 4$ and for higher $\alpha \ge 6$ it reduces in the flow region except in the vicinity of y=-1. Whole |v| enhances with $|\alpha| \ge 6$. Fig.8 shows that |v| fluctuates in the left half and reduces in the right half with increased in $x + \gamma t$.

The non-dimensional temperature (θ) is exhibited in figs 9 – 12 for different values of $G, R, D^{-1}, \alpha, \gamma$ and $x+\gamma t$. It is found from fig 9 that the actual temperature enhances with increase in G>0 and reduces with G<0. From fig. 10 the behavior of θ with D^{-1} shows that lesser the permeability of the porous medium larger the actual temperature in the flow field and for further lowering of the permeability smaller the temperature in the region. Also an increase in γ enhances θ in the flow region. We find that higher the Reynolds number R larger the actual temperature in the flow region. From fig 11 the variation of θ with heat source parameter α shows that θ is positive for α >0, and for $\alpha < 0$, θ is negative in the central region and positive in the region adjacent to y $=\pm 1$. We find that the actual temperature enhances with increase in the strength of the heat source and for α <0 the actual temperature experiences a depreciation. Fig. 12 shows that the actual temperature reduces with phase $x+\gamma t \le \pi$ and enhances with higher $x+\gamma t \ge 2\pi$.

The shear stress (τ) at the walls y $=\pm 1$ have been evaluated for different variations in $G, R, D^{-1}, \alpha, \gamma$ and $x+\gamma t$ are shown in tables 1 – 6. It is found that the stress at y $=\pm 1$ decreases with G>0 and enhances with G<0 at $D^{-1}=10^2$ while a reversal effect is noticed at higher $D^{-1} \ge 2\times 10^2$, while at y=-1, the stress enhances with G>0 and reduces with G<0 for all D^{-1}. Lesser the permeability of the porous medium larger the magnitude of the stress at both the walls in both heating and cooling cases and for further lowering of the permeability it reduces for G>o and enhances for G<0 at y= 1.where as a reversed effect is noticed at y=-1. An increase in the thermal wave velocity γ depreciates $|\tau|$at y=-1 and enhances at y=1. The variation of τ with an increase in R reduces $|\tau|$ for G>0 and enhances it for G<0 while at y=1, $|\tau|$ reduces with R$\le$70 for G>0 and enhances for G<0. While for higher R$\ge$140,$|\tau|$enhances for G>0 and reduces for G<0 at both the walls. $|\tau|$enhances with$|\alpha|$for G>0 and reduces with $|\alpha|$for G<0 at y$=\pm 1$. The variation of τ with the phase $x+\gamma t$ reveals that the stress at y=1 depreciates for G>0 and enhances for G<0 for $x+\gamma t \le \frac{\pi}{2}$ and for higher values of $x+\gamma t \ge 2\pi$, $|\tau|$ enhances for G>0 and reduces for G<0 at y $=\pm 1$.

The Nusselt Number Nu at y$=\pm 1$ is shown in tables 7 - 12 for different values of G, D^{-1}, α, γ and $x+\gamma t$. It is found that the rate of heat transfer at y $=\pm 1$ reduces with increase in G>0 at $D^{-1}=10^2$ and at higher $D^{-1} \ge 2\times 10^2$, Nu enhances for G>0 and reduces for G<0 while at y=-1 it increases with when $D^{-1}=10^2$ and decreases when $D^{-1} \ge 2\times 10^2$ with G<0. The variation of Nu with D^{-1} shows that |Nu| depreciate with $D^{-1} \le 2\times 10^2$ for G>0 and reduces for G<0 at both the walls, and enhances with $D^{-1} \ge 3\times 10^2$ at y=1 and reduces at y=-

1. An increase in Reynolds Number R enhances |Nu| at y= ± 1 for |G|=10^3 and reduces for $|G|=3\times10^3$ while at y=-1, |Nu| enhances for all G. An increase in γ reduces Nu at y=+1and enhances at y=-1. The variation of Nu with heat source parameter α shows that |Nu| at y=1 enhances for $\alpha \geq 6$, Nu enhances at |G|=10^3 and reduces at $D^{-1}=3\times10^2$ with increases in α >4 and in the case of α <0 it enhances with $|\alpha| \leq 4$ and for $|\alpha| \geq 6$ it enhances for G>0 and reduces for G<0. At y=-1 the rate of heat transfer depreciates with $\alpha \geq 0$ at |G|= 10^3 and enhances at $|G|=3\times10^3$ and it reduces with increase in $\alpha < 0$ in both heating and cooling cases. The variation of Nu with phase $x+\gamma t$ show that |Nu| experiences an enhancement with increase in $x+\gamma t \leq \pi$ and for higher values of $x+\gamma t \leq 2\pi$ it depreciates for all G at both the walls. In general we notice that the rate heat transfer y=+1 is greater than that at y=-1.

BIBLIOGRAPHY

1	Bharathi, M,	Hydrodynamic Mixed convective Heat transfer through a porous medium in channels / pipes with Radiation effect, Ph.D., thesis, S.K.University, Anantapur,	2009
2	Goren, S.L,	On free convection in water at 4°C. Chem. Engg. Sci. V.21, p.515.,	1966
3	Govindaraju,	J, Chem. Engng. Sci., 25, pp. 18-27,	1970
4	Jaiswal, B.S and Soundalegekhar, V.M,	Oscillating plate temperature effects on the flow past on infinite vertical porous with constant and embedded in porous medium τ Heat mass transfer V. 37, pp. 125-131,	2001
5	Jafarunnisa,	Unsteady hydro magnetic mixed convection flow in a vertical channel with traveling thermal wave and quadratic temperature variation. M.Phil dissertation, S.K. University, Anantapur, (India) ,	2009
6	Kaviany, M,	Principles of the heat transfer in a porous medium 2nd edn. Springer-Verlag New York,	1999
7	Raptis, A.A,	Flow through a porous medium in the presence of magnetic field Int. J. Energy Research, V. 10, pp. 97-100,	1986

8	Ravindra, M,	MHD convection flow through porous medium with non-uniform wall temperature, Ph.D. thesis, SKU, Anantapur (India),	1994
9	Vajravelu, K, and Debnath, L,	Non-linear study of convective heat transfer and fluid flows induced by traveling thermal wave, Acta mech, V. 59, pp. 233-249,	1986
10	Whitehead, J.A,	Geo-physics, fluid dynamics, V. 3, pp. 161-180,	1972

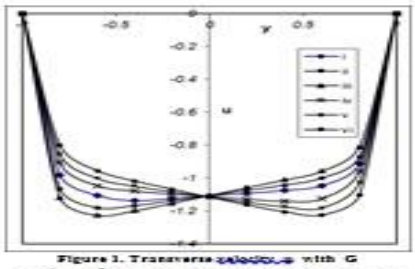

Figure 1. Transverse velocity with G

$D^{-1} = 10^2, \alpha = 2, y = 5, x + yt = \pi/4, R = 35$

	i	ii	iii	iv	v	vi
G	10^2	3×10^2	5×10^2	-10^2	-3×10^2	-5×10^2

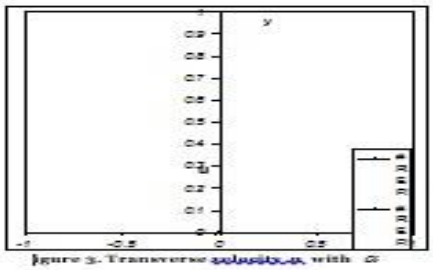

Figure 3. Transverse velocity with α

	i	ii	iii	iv	v	vi
α	2	4	6	-2	-4	-6

$G = 10^2, D^{-1} = 10^2, y = 5, x + yt = \pi/4, R = 35$

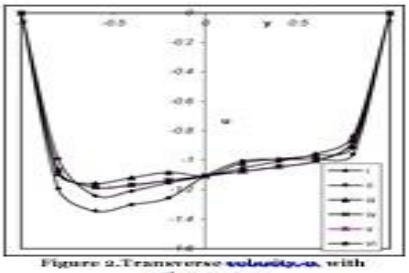

Figure 2. Transverse velocity with D^{-1}, y and R

$G = 10^2, \alpha = 2, x + yt = \pi/4$

	i	ii	iii	iv	v	vi
D^{-1}	10^2	2×10^2	3×10^2	10^2	10^2	10^2
y	5	5	5	10	5	5
R	35	35	35	35	70	140

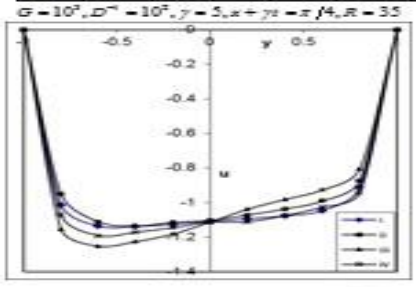

Figure 4. Transverse velocity with $x + yt$

$G = 10^2, D^{-1} = 10^2, \alpha = 2, y = 5, R = 35$

	i	ii	iii	iv
$x+yt$	$\pi/4$	$\pi/2$	π	2π

PUNE RESEARCH DISCOVERY ISSN 2455-9202
AN INTERNATIONAL JOURNAL OF ADVANCED STUDIES VOL 2, ISSUE 2

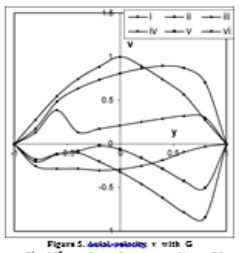

Figure 5. Axial velocity v with G
$D^{-1}=10^2, \alpha=2, y=5, x+y_1=\pi/4, R=35$

G	I	II	III	IV	V	VI
	10^2	3×10^2	5×10^2	-10^2	-3×10^2	-5×10^2

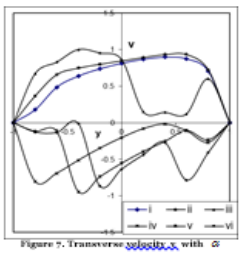

Figure 7. Transverse velocity u with α
$G=10^2, D^{-1}=10^2, y=5, x+y_1=\pi/4, R=35$

	I	II	III	IV	V	VI
α	2	4	6	-2	-4	-6

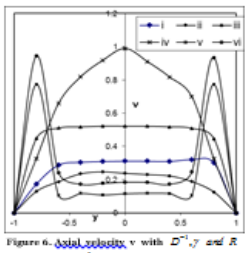

Figure 6. Axial velocity v with D^{-1}, y and R
$G=10^2, \alpha=2, x+y_1=\pi/4$

	I	II	III	IV	V	VI
D^{-1}	10^2	2×10^2	3×10^2	10^2	10^2	10^2
γ	5	5	5	10	5	5
R	35	35	35	35	70	140

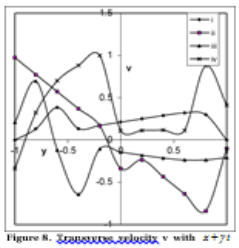

Figure 8. Transverse velocity v with $x+y_1$
$G=10^2, D^{-1}=10^2, \alpha=2, y=5, R=35$

	I	II	III	IV
$x+y_1$	$\pi/4$	$\pi/2$	π	2π

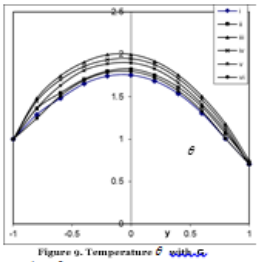

Figure 9. Temperature θ with G
$D^{-1}=10^2, \alpha=2, y=5, x+y_1=\pi/4, R=35$

	I	II	III	IV	V	VI
G	10^2	3×10^2	5×10^2	-10^2	-3×10^2	-5×10^2

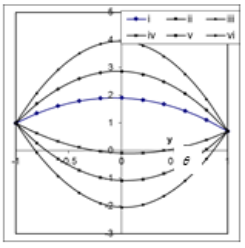

Figure 11. Temperature θ with α
$G=10^2, D^{-1}=10^2, y=5, x+y_1=\pi/4, R=35$

	I	II	III	IV	V	VI
α	2	4	6	-2	-4	-6

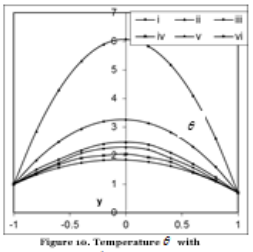

Figure 10. Temperature θ with
D^{-1}, y and R
$G=10^2, \alpha=2, x+y_1=\pi/4$

	I	II	III	IV	V	VI
D^{-1}	10^2	2×10^2	3×10^2	10^2	10^2	10^2
γ	5	5	5	10	5	5
R	35	35	35	35	70	140

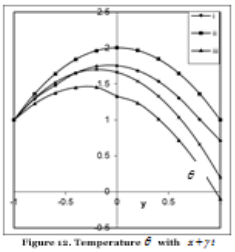

Figure 12. Temperature θ with $x+y_1$
$G=10^2, D^{-1}=10^2, \alpha=2, y=5, R=35$

	I	II	III	IV
$x+y_1$	$\pi/4$	$\pi/2$	π	2π

Table 1
shear stress $[\tau]_{y=\frac{1}{2}}$, $\alpha=2, x+y_1=\pi/4, R=35$

G	I	II	III	IV	V	VI
10^2	-11.20456	-15.67265	-12.37778	-11.21515	-11.22507	-11.24567
3×10^2	-11.42943	-14.13072	0.27633	-11.42943	-11.47655	-11.55059
-10^2	-11.01075	-15.55615	-24.60522	-11.01176	-11.00012	-10.97579
-3×10^2	-10.82993	-16.32902	-37.05554	-10.83093	-10.80667	-10.76013
D^{-1}	10^2	2×10^2	3×10^2	10^2	10^2	10^2
γ	5	5	5	10	5	5
R	35	35	35	35	70	140

Table 2
shear stress $[\tau]_{y=\frac{1}{2}}$, $\alpha=2, x+y_1=\pi/4, R=35$

G	I	II	III	IV	V	VI
10^2	11.12744	15.45691	24.18463	11.12214	11.12573	11.14668
3×10^2	11.14369	16.46271	25.93778	11.14349	11.13857	11.11193
-10^2	11.09097	14.79780	12.52893	11.09067	11.09089	11.07696
-3×10^2	11.03444	13.95131	0.82048	11.03434	11.03915	11.00780
D^{-1}	10^2	2×10^2	3×10^2	10^2	10^2	10^2
γ	5	5	5	10	5	5
R	35	35	35	35	70	140

Table 3
Nusselt number $[Nu]_{y=\frac{1}{2}}$, $\alpha=2, x+y_1=\pi/4, R=35$

G	I	II	III	IV	V	VI
10^2	2.03254	1.03201	1.50560	2.03284	2.37570	2.54053
3×10^2	2.14108	2.56023	2.71301	2.12108	1.69956	1.35320
-10^2	2.50286	2.04004	2.05008	2.50286	4.04141	5.46143
-3×10^2	2.11243	2.54169	2.69554	2.11243	1.62553	1.16569
D^{-1}	10^2	2×10^2	3×10^2	10^2	10^2	10^2
γ	5	5	5	10	5	5
R	35	35	35	35	70	140

Table 4
Nusselt number $[Nu]_{y=\frac{1}{2}}$, $\alpha=2, x+y_1=\pi/4, R=35$

G	I	II	III	IV	V	VI
10^2	-0.00123	-0.79397	-0.77425	-0.08879	-0.14253	-0.29143
3×10^2	-0.05173	-0.05809	-0.05459	-0.09173	-0.13015	-0.18509
-10^2	-0.13222	-0.10411	-0.09734	-0.14222	-0.25015	-0.63530
-3×10^2	-0.18254	-0.07532	-0.07449	-0.08254	-0.09992	-0.14144
D^{-1}	10^2	2×10^2	3×10^2	10^2	10^2	10^2
γ	5	5	5	10	5	5
R	35	35	35	35	70	140

Table 5
shear stress $[\tau]_{y=\frac{1}{2}}$, $D^{-1}=10^2, y=5, x+y_1=\pi/4, R=35$

G	I	II	III	IV	V	VI
10^2	-11.20456	-11.72598	-12.60469	-11.15772	-11.61105	-12.37784
3×10^2	-11.42943	-13.12454	-15.99256	-11.23926	-12.52457	-14.63470
-10^2	-11.01075	-10.49324	-9.65595	-11.08525	-10.59957	-9.79336
-3×10^2	-10.82993	-9.40070	-7.19155	-10.96525	-9.45717	-8.54574
α	2	4	6	-2	-4	-6

Table 6
shear stress $[\tau]_{y=\frac{1}{2}}$, $D^{-1}=10^2, y=5, x+y_1=\pi/4, R=35$

G	I	II	III	IV	V	VI
10^2	11.12744	11.55890	12.30527	11.12111	11.77906	12.67010
3×10^2	11.14369	12.24903	14.25412	11.47500	13.19045	16.04831
-10^2	11.09097	10.84640	9.86350	10.98903	10.45444	9.80538
-3×10^2	11.03444	9.80206	7.00765	10.76047	9.22763	8.58053
α	2	4	6	-2	-4	-6

Table 7
Nusselt number $[Nu]_{y=\frac{1}{2}}$, $D^{-1}=10^2, y=5, x+y_1=\pi/4, R=35$

G	I	II	III	IV	V	VI
10^2	2.03254	7.04267	-9.79150	-2.57491	-2.87529	-2.94947
3×10^2	2.14108	2.34295	1.75015	-2.05483	-6.99942	10.98375
-10^2	2.50286	2.81930	-4.90192	-1.55237	-3.02612	-2.73379
-3×10^2	2.11243	2.24769	1.72248	-2.15051	-10.91401	6.22967
α	2	4	6	-2	-4	-6

Table 8
Nusselt number $[Nu]_{y=\frac{1}{2}}$, $D^{-1}=10^2, y=5, x+y_1=\pi/4, R=35$

G	I	II	III	IV	V	VI
10^2	-0.00123	0.00749	-0.16379	-0.14795	-0.05355	0.01676
3×10^2	-0.05173	-0.05145	-0.07059	-0.09515	-0.05837	-0.04597
-10^2	-0.13222	-0.64529	0.73651	-0.09925	-0.06404	-0.04551
-3×10^2	-0.18254	-0.00584	0.00983	-0.07657	-0.03033	-0.02229
α	2	4	6	-2	-4	-6

PUNE RESEARCH DISCOVERY ISSN 2455-9202
AN INTERNATIONAL JOURNAL OF ADVANCED STUDIES VOL 2, ISSUE 2

Table – 9

shear stress $[\tau]_{y=1}$, $D^{*}=10^{2}, \gamma=5, \alpha=2, R=35$

G	i	ii	iii	iv
10^{2}	-11.20456	-11.29392	-11.04454	-11.09920
3×10^{2}	-11.42941	-11.66804	-10.90535	-11.07035
-10^{2}	-11.01075	-10.92639	-11.18625	-11.13722
-3×10^{2}	-10.82991	-10.55734	-11.26224	-11.20556
$x+7i$	$\pi/4$	$\pi/2$	π	2π

Table – 10

shear stress $[\tau]_{y=1}$, $D^{*}=10^{2}, \gamma=5, \alpha=2, R=35$

G	i	ii	iii	iv
10^{2}	11.12744	11.14668	11.03912	11.05215
3×10^{2}	11.14269	11.21192	10.89596	11.03662
-10^{2}	11.09097	11.07696	11.19579	11.13591
-3×10^{2}	11.03444	11.00780	11.27569	11.13926
$x+7i$	$\pi/4$	$\pi/2$	π	2π

Table – 11

Nusselt number $[Nu]_{y=1}$, $D^{*}=10^{2}, \gamma=5, \alpha=2, R=35$

G	i	ii	iii	iv
1.00	2.02354	2.20139	-5.52835	2.67360
2.00	2.14108	2.00251	-2.74522	2.53478
-1.00	2.50286	1.99995	-11.58217	11.38837
-2.00	2.11242	1.99582	-2.56051	2.40021
$x+7i$	$\pi/4$	$\pi/2$	π	2π

Table – 12

Nusselt number $[Nu]_{y=1}$, $D^{*}=10^{2}, \gamma=5, \alpha=2, R=35$

G	i	ii	iii	iv
1.00	-0.00123	0.03207	0.19415	-0.10702
2.00	-0.05173	0.00003	0.29705	-0.09222
-1.00	-0.13222	0.00000	0.17921	-0.15559
-2.00	-0.18254	0.00007	0.32949	-0.08412
$x+7i$	$\pi/4$	$\pi/2$	π	2π

(Ctrl)